

Article

# Investigation of Soil Heaving and Penetration Resistance of Bucket Foundation with Inner Bucket and Cruciform Skirts

Zhong Xiao <sup>1,\*</sup>, Teng Ma <sup>1</sup>, Hongwei Wang <sup>2</sup>, Feng Bian <sup>2</sup>, Haifeng Jin <sup>2</sup>, Tengjiao Yu <sup>2</sup>, Wei Zhang <sup>1</sup>, Pan Hu <sup>3,\*</sup>  and Jinhui Li <sup>4</sup>

<sup>1</sup> State Key Laboratory of Hydraulic Engineering Simulation and Safety, Tianjin University, Tianjin 300072, China

<sup>2</sup> Shallow Water Development Company, PetroChina Dagang Oilfield Company, Tianjin 300280, China

<sup>3</sup> School of Engineering, Design and Built Environment, Western Sydney University, Sydney 2747, Australia

<sup>4</sup> Department of Civil and Environmental Engineering, Harbin Institute of Technology (Shenzhen), Shenzhen University Town, Shenzhen 518055, China

\* Correspondence: tjzhongxiao@tju.edu.cn (Z.X.); p.hu@westernsydney.edu.au (P.H.)

**Abstract:** Since concrete is cheaper and more resistant to corrosion than steel, the wide-shallow concrete bucket foundation is being used extensively in ocean engineering. By adding the inner bucket and cruciform skirts, both the bearing capacity and rigidity of the wide-shallow concrete bucket foundation increase significantly. When compared to the hollow steel bucket foundation, the inclusion of thicker skirts, as well as the addition of inner bucket and cruciform skirts, would cause changes to the soil flow mechanism, resulting in soil heave within each compartment and changes in soil strength evolution and penetration resistance during installation in clay. In order to study the influence of the addition of the inner bucket and cruciform skirts on the soil heaving inside each compartment, soil softening and penetration resistance, three-dimensional large deformation finite element (LDFE) models for the bucket foundation with and without inner bucket, and cruciform skirts considering soil remolding were established using the Coupled Eulerian–Lagrangian (CEL) approach. It was found that the inner bucket significantly changes the soil flow and softening of the soil during penetration of the bucket foundation. According to the theoretical analysis and numerical results, the diameter of the optimal inner bucket is equal to 5/8 of the outer diameter. The adhesion coefficient observed in this study falls within the range of 0.5 to 0.8, which is higher than the theoretical value of 0.25 that assumes the soil is fully remolded. The reason for this discrepancy is that the soil is only partially remolded during the actual installation of the bucket foundation. The neglect of the softening of the soil or considering the soil as completely softened will result in significant variation in the predicted penetration resistance; hence, partial softening of the soil should be taken into account.

**Keywords:** wide-shallow concrete bucket foundation; inner bucket and cruciform skirts; soil heaving; penetration resistance; soil remolding; optimal value



**Citation:** Xiao, Z.; Ma, T.; Wang, H.; Bian, F.; Jin, H.; Yu, T.; Zhang, W.; Hu, P.; Li, J. Investigation of Soil Heaving and Penetration Resistance of Bucket Foundation with Inner Bucket and Cruciform Skirts. *J. Mar. Sci. Eng.* **2023**, *11*, 996. <https://doi.org/10.3390/jmse11050996>

Academic Editor: Antoni Calafat

Received: 10 February 2023

Revised: 26 April 2023

Accepted: 5 May 2023

Published: 7 May 2023



**Copyright:** © 2023 by the authors. Licensee MDPI, Basel, Switzerland. This article is an open access article distributed under the terms and conditions of the Creative Commons Attribution (CC BY) license (<https://creativecommons.org/licenses/by/4.0/>).

## 1. Introduction

Due to the advantages of lower cost and better durability, the wide-shallow concrete bucket foundation has a great potential in coastal and ocean engineering, and it can be used as the foundation of an offshore deep-water wharf, breakwater, or offshore wind turbine. Normally, the rigidity of the wide-shallow concrete bucket foundation is relatively small due to its large diameter and shallow penetration depth. However, by adding the inner bucket and cruciform skirts, both the bearing capacity and rigidity of the bucket foundation will increase significantly [1]. A typical application of such a configuration is a deep-water wharf, as shown in Figure 1.

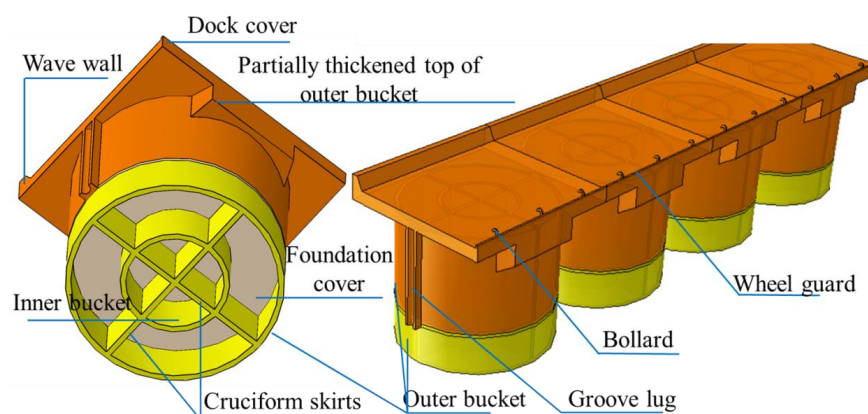


**Figure 1.** The deep-water wharf using bucket foundation with inner bucket and cruciform skirts.

The inner bucket and cruciform skirt significantly increase the total area of the bottom and skirt; therefore, the foundation will be subjected to larger penetration resistance during its installation process. In addition, soil heaving will occur in each compartment separated by the inner bucket and cruciform skirt, which may prevent the foundation from reaching the designed installation depth and affect its post-installation bearing capacity. However, current research on the installation of bucket foundations mainly focuses on the ones with no compartment. The bucket foundation was first applied in an actual engineering project in 1994, and Tjelta [2], through research on the measured data, found that installation methods, including self-weight penetration, pressing penetration, and suction-assisted penetration, have a significant impact on the soil flow mechanism. Iskander et al. [3] conducted 1g indoor experiments on the penetration and extraction behavior of suction bucket foundations in clay and sand and explained the variation of penetration resistance and soil heaving. Chen et al. [4] focused on the influence of different installation methods on the penetration process and installation effect of bucket foundations, studying the impact of different installation methods on the penetration process. Zhai et al. [5] also analyzed how to reduce penetration resistance through indoor experiments. Wang et al. [6] used the arbitrary Lagrangian–Eulerian (ALE) method to simulate the installation process of suction buckets and compared the difference in penetration resistance and soil heaving under different installation methods. Xiao et al. [7] studied the changes in penetration resistance and soil flow mechanism during the penetration process of a single bucket foundation, considering the strain softening and rate effect of soil using the coupled Eulerian–Lagrangian (CEL) method. The adverse effects of bucket penetration-induced soil heaving and softening on the ultimate bearing capacity were also studied [8]. Jin et al. [9] used the smoothed particle hydrodynamics (SPH) method to simulate the penetration process of bucket foundations in sand.

There have been few studies on bucket foundations with multiple compartments, mostly focusing on on-site or indoor experiments. Liu et al. [10] studied a new type of seven-compartment suction bucket shallow foundation (CBSF) used in a wind farm project in Jiangsu, China. Zhang et al. [11] conducted a large-scale model study on the installation speed, penetration resistance, and levelness of the foundation in typical saturated silty clay for the seven-compartment suction bucket.

However, overall, there is still a lack of relevant research using three-dimensional large deformation numerical simulation methods to simulate the penetration process of bucket foundations with internal buckets and cruciform skirts in soil and analyze the penetration resistance and soil flow characteristics with consideration of soil softening properties.

When the ratio of the diameter of the inner bucket to that of the outer bucket changes, the height of soil heave inside each compartment during the installation process may vary accordingly. As the foundation cover contacts the heaved soil inside the compartment, sinking of the foundation will be halted. In such case, the soils within some compartments are still not in contact with the foundation cover after installation, which will obviously

reduce the post-installation vertical bearing capacity of the foundation. Therefore, it is necessary to study soil heaving and penetration resistance during the installation of a bucket foundation with inner bucket and cruciform skirts in clay considering soil remolding under different ratios of the diameter of the inner bucket to that of the outer bucket. The bucket foundation with inner bucket and cruciform skirts has the optimal ratio of the diameter of the inner bucket to that of the outer bucket when the height of the soil heaving in the inner and outer compartments is almost equal after installation.

Large deformation numerical analysis is required to model the installation of the bucket foundation with inner bucket and cruciform skirts in clay. In the literature, there are three large deformation numerical methods by which to simulate the installation of the bucket foundation in clay; these include the ALE method [7], the remeshing and interpolation technique by small strain (RITSS) [8], and the CEL method [7]. For the ALE method, a new mesh is created when the elements have obvious distortion. Then, the variables are mapped from the old mesh to the new mesh, which can accurately define material boundaries and complex contact interactions. However, it is mostly applied to solve plane strain or axisymmetric problems due to the limitation of computational efficiency. The RITSS method falls into the category of the ALE method in nature [12], but the topological relationship between its old mesh and new mesh can be changed. Nevertheless, it requires the user to write a program to implement the entire calculation process, and the realization of the interpolation of the variables from the old mesh to the new mesh is challenging. The CEL method is a new finite element analysis method for large deformations, which combines the Eulerian analysis method and Lagrangian analysis method. As the CEL method can better simulate the deformation of the material in the Eulerian mesh, it can effectively solve the large deformation problems such as mesh and element distortions in the traditional Lagrangian domain [13].

In this study, a three-dimensional large deformation finite element model incorporating the effect of soil remolding was established to model the installation of a bucket foundation with inner bucket and cruciform skirt in clay using the CEL method. The influences of the inner bucket and cruciform skirts on the soil heaving and penetration resistance during the installation of the bucket foundation in clay were analyzed and discussed. Meanwhile, the evolution of soil remolding at different penetration depths was demonstrated. The contribution of the resistance from each component of the foundation to the total penetration resistance was analyzed. The optimal ratio of the diameter of the inner bucket to that of the outer bucket was proposed based on theoretical analysis and validated by the numerical results. Key findings were obtained and discussed from the numerical results, and recommendations were made.

## 2. Method and Materials

### 2.1. Finite Element Mesh and Boundary Conditions

The CEL large deformation finite element analysis method in commercial software Abaqus is used to simulate the penetration of the concrete bucket foundation with inner bucket and cruciform skirts. It is commonly used to solve geomechanical boundary value problems involving large deformations. The CEL method adopts an explicit time integration scheme with the central difference rule for the solution of the non-linear system of differential equations. No iteration is needed as the unknown solution for the next time step can be found from the solution of the previous time step. In the CEL formulation, the Lagrangian domain deals with the deformations of the bucket foundation and the Eulerian domain deals with the displacement of the soil. The numerical model only contains the eight-node Eulerian elements (EC3D8R), which are the only available elements in CEL analyses. Displacement boundary conditions were applied to the bucket foundation through a reference point.

For concrete bucket foundation, the common sizes of  $D$  typically range from 5 to 25 m, with  $t$  falling within the range of 0.2 to 0.6 m. Therefore, the outer diameter of the outer bucket ( $D$ ) is set as 10 m, while the diameter of the inner bucket ( $D_{in}$ ) in the base is equal to

$D/2$ . A typical value of  $t = 0.4$  m is used for all the skirt thickness. In order to avoid the influence of soil boundary effect on the penetration process, the radius of the soil domain is set to  $3D$  and the soil depth is set to  $5D$ . The height of the Eulerian mesh needs to exceed the original top boundary of the soil to avoid the loss of the material. A 5 m void layer was set above the soil field to allow sufficient flow space of the surface soil. In order to maintain the accuracy of the calculation of the penetration resistance and soil heaving in the bucket, a very fine mesh zone shaped in a square column with width of  $1.25D$  was set surrounding the bucket foundation. The minimum mesh size was set as  $t/6$ , as shown in Figure 2, which is consistent with the setting in Xiao et al. (2019) [7]. Due to the symmetry, and in order to improve the computational efficiency, only a quarter of the domain was selected for the simulation, as shown in Figure 2. The soil base was fixed while only vertical displacements were allowed for side boundaries.

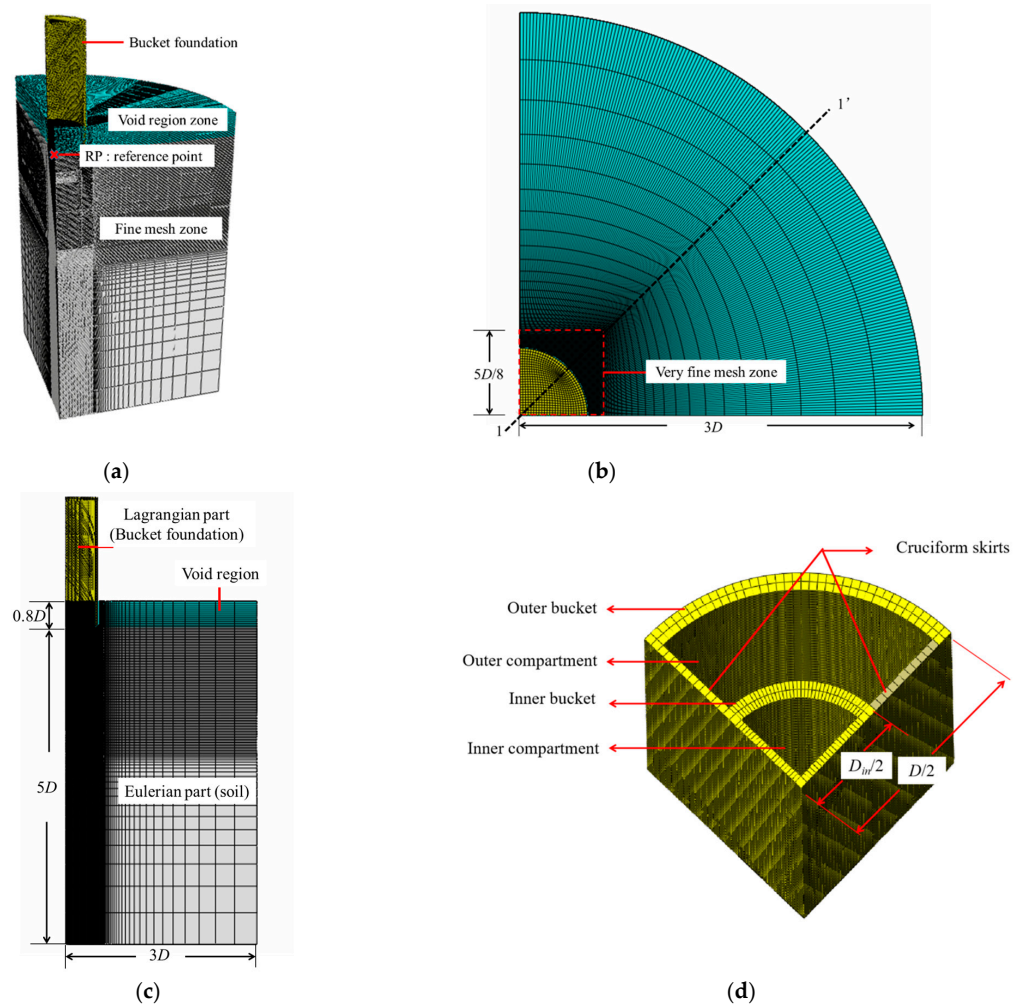


**Figure 2.** Geometry and mesh of the 3D CEL model. (a) 3D view. (b) Top view. (c) Side view. (d) Details of the bucket foundation.

### 2.2. Contact and Penetration Rate

In the CEL finite element model, the contact between the soil and the foundation adopted a universal contact surface based on the penalty contact method. The contact force is calculated using the normal and tangential components of the displacement and the friction coefficient. The normal component of the contact force acts to prevent penetration between the surfaces, while the tangential component of the contact force acts to prevent sliding between the surfaces. It aims to model an undrained behavior, as the soil always sticks to the bucket foundation while failure occurs within the soil. A sufficiently large friction coefficient  $\mu$  was adopted so that the sliding failure occurs on the soil element

adjacent to the bucket wall. The result of the case when  $\mu = 0.2$  is the same as that of the case when  $\mu = 10$ . Therefore,  $\mu$  is set as 0.2 to ensure that sliding failure occurs on the soil elements adjacent to the bucket wall.

The bucket foundation can be installed using suction or jacking after self-weight penetration. In this study, the caisson was penetrated into the soil at a constant rate using velocity control to model the jacking installation of the bucket foundation with inner bucket and cruciform skirts. A penetration rate of 1 m/s was adopted for the installation of the bucket foundation, which provides a good balance between the accuracy and efficiency of the simulation (Xiao et al., 2019) [7].

### 2.3. Material Properties

The bucket foundation with inner bucket and cruciform skirts was simulated as a rigid body as its rigidity is much greater than that of clay. The saturated clay was modeled by an ideal elastoplastic constitutive model based on the Tresca yield criterion. The gradient of the undrained shear strength of clay with depth  $z$  is usually 1–2 kPa/m [14–17]; hence, the undrained shear strength of the clay was prescribed with  $s_u = 2 + 1.2z$  in this study. The effective unit weight of the clay was adopted as  $\gamma' = 6.5 \text{ kN/m}^3$ , which is also a typical value for marine soft soil [15,17]. The elastic modulus  $E$  of the soil was set as  $500s_u$  [18,19]. The Poisson’s ratio  $\nu$  was 0.499 [18,19], which is used to simulate the volume incompressibility of the saturated soft soil under undrained conditions.

In order to simulate the remolding of the soil, the softening model [20] and rate effect model [21] were combined with the Tresca yield criterion to describe the evolution of the undrained strength of clay. During the penetration, the soil is disturbed and therefore undergoes softening. Meanwhile, when the shear strain rate is higher than the reference strain rate, the shear strength of the soil will increase, which is termed the strain rate effect of the soil. Both of these factors act on the strength of the soil simultaneously. Therefore, the equation for calculating the undrained shear strength considering the strain softening and rate effects of marine soft soil is expressed as follows:

$$s_u = \beta_s \beta_r s_{u0} \tag{1}$$

where

$$\beta_s = \delta_{rem} + (1 - \delta_{rem})e^{-3\zeta/\zeta_{95}} \tag{2}$$

and

$$\beta_r = \left[ 1 + \eta \left( \frac{\max(\dot{\gamma}, \dot{\gamma}_{ref})}{\dot{\gamma}_{ref}} \right)^\beta \right] / (1 + \eta) \tag{3}$$

where  $s_u$  is the shear strength of clay after considering the softening and rate effects;  $s_{u0}$  is the initial soil shear strength;  $\beta_s$  is the softening effect coefficient, while  $\beta_r$  is the rate effect coefficient;  $\delta_{rem}$  is the ratio of the initial shear strength of the clay to the shear strength when the soil is completely disturbed, and its value is equal to the inverse of the soil sensitivity  $S_t$ ;  $\zeta$  is the accumulated absolute plastic shear strain;  $\zeta_{95}$  is the accumulated shear strain corresponding to the 95% degradation in soil strength from intact to fully-remolded conditions; and  $\eta$  and  $\beta$  represent the viscosity characteristics and shear index of the soil, respectively, and the general values range from 0.1 to 2.0 and 0.05 to 0.2, respectively. The  $\dot{\gamma}_{ref}$  is the reference shear strain rate, and  $\dot{\gamma}$  is the maximum shear strain rate, which is calculated by:

$$\dot{\gamma} = \frac{\Delta\varepsilon_1 - \Delta\varepsilon_3}{\Delta t} \tag{4}$$

where  $\Delta\varepsilon_1$  and  $\Delta\varepsilon_3$  are the cumulative major and minor principal strains over the duration of  $\Delta t$ .

For marine clays, the commonly used values for soil sensitivity  $S_t$  and ductility coefficient  $\zeta_{95}$  are 2–6 and 10–50, respectively [20,22]. The soil sensitivity  $S_t = 4$  and the ductility coefficient  $\zeta_{95} = 30$  were taken in this study.

Some assumptions have been made on the numerical model: the distribution of soil strength is assumed to increase proportionally with depth; all lateral frictional resistance is believed to occur within the soil itself, as opposed to at the interface between the soil and the bucket wall; and finally, the bucket is assumed to be penetrated at a constant speed.

### 2.4. Model Validation

The CEL model was initially validated against the centrifuge test results reported for the jacking installation of the bucket foundation [16,23]. The sizes of the bucket foundations are shown in Figure 3. The undrained shear strength of the soil is  $s_{u0} = 1.25z$  kPa and  $s_{u0} = 10 + 2.8z$  kPa in validation case 1 and 2, respectively. The corresponding details of the foundation dimensions and soil properties are shown in Table 1. The comparison of the penetration resistance obtained from the CEL analysis in this study and the centrifuge testing results [16,23] can be seen in Figure 3, where  $d_p$  is the penetration depth of the bucket foundation relative to the mud surface. For both cases, reasonably good agreement can be found with the maximum difference less than 15%. The root mean square error (RMSE) for comparison of the penetration resistances in Chen et al. (2007) and Westgate et al. (2009) are approximately 0.2 and 0.05, respectively. The relatively close results confirm the validity of the CEL model in this study.

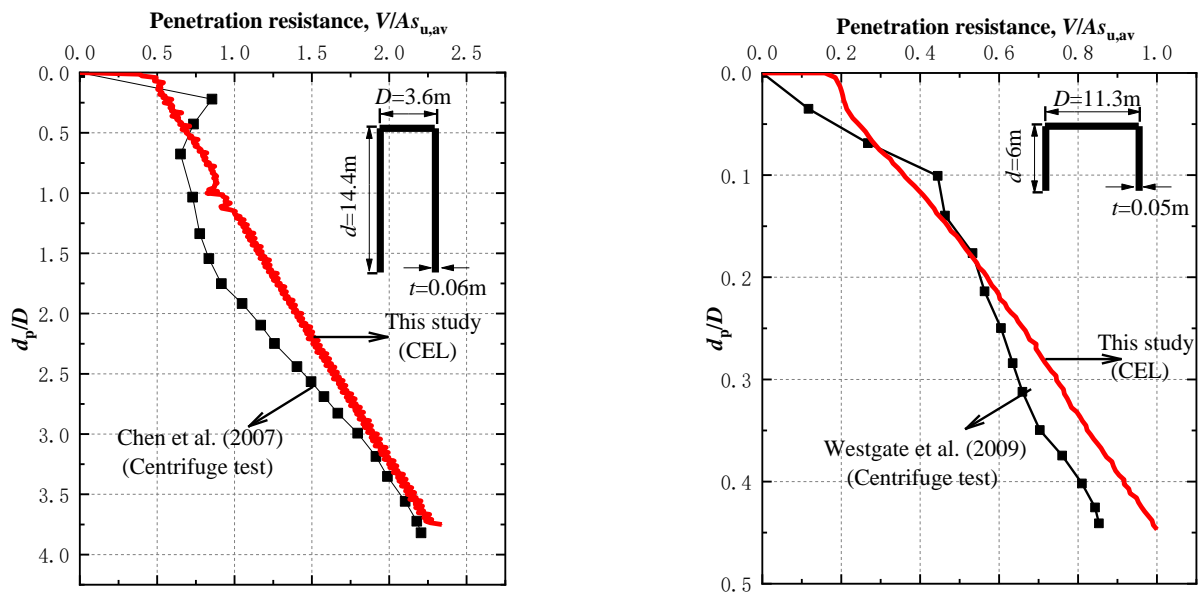


Figure 3. Comparison of the penetration resistance between the CEL analysis results and centrifuge test results [16,23].

Table 1. Details of the foundation dimensions and soil properties in validation cases.

Case	$\gamma'$ (kN/m <sup>3</sup> )	$S_t$	$\zeta_{95}$	$\eta$	$\beta$	$E/s_u$	$s_{u0}$ (kPa)	$D$ (m)	$d$ (m)	$t$ (m)	Reference
Case 1	6.7	2.6	10	1	0.1	500	$1.25z$	3.6	14.4	0.06	[Chen et al. (2007) [16]]
Case 2	5.9	3	10	1	0.1	500	$10 + 2.8z$	11.3	6	0.05	[Westgate et al. (2009) [23]]

## 3. Numerical Results

### 3.1. Soil Flow and Heaving in Each Compartment

During the penetration of the bucket foundation, the soil will be squeezed by the skirts; therefore, the height of the soil surface inside the bucket will vary. If soil heaving happens inside the bucket, the foundation cannot be installed to the predetermined design depth. As a consequence, the actual bearing capacity will be less than the design bearing capacity.

The average height of the soil surface inside the bucket foundation relative to the original mud surface is defined as  $H_{plug}$ . If it is positive, it indicates that the soil surface

inside the bucket is higher than the original mud surface. Otherwise, the soil inside the bucket settles. Take the base case ( $D_{in} = D/2$ ) as an example; the comparison of  $H_{plug}$  in the inner or outer compartment of the bucket foundation with and without inner bucket and cruciform skirts at different penetration depth ratio ( $d_p/D$ ) is shown in Figure 4.

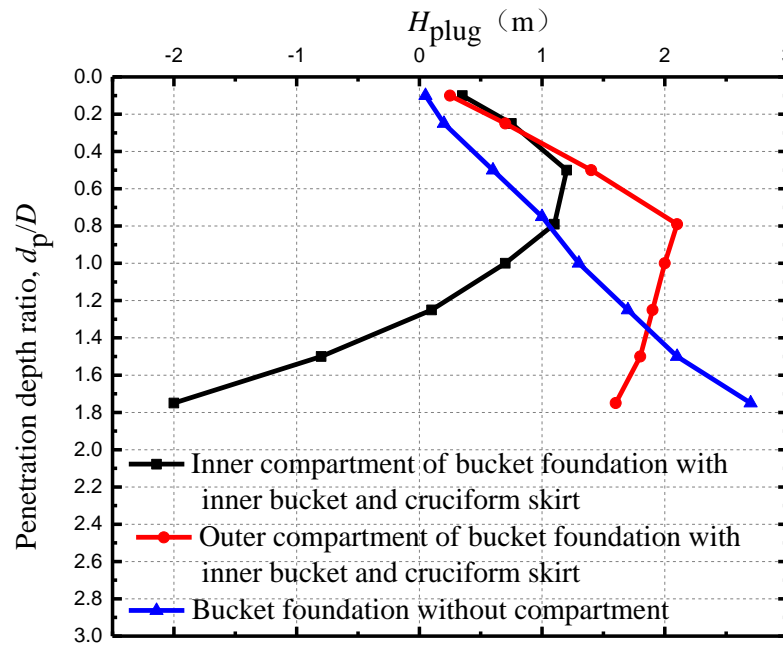


Figure 4. Average height of soil surface at different penetration depth ratio.

It can be seen from Figure 4 that the height of the soil surface in the bucket foundation without compartment continuously increases with the penetration depth ratio. With the increase of the penetration depth ratio, the soils displaced by the skirt are inclined to flow into the bucket. This is because the earth pressure within the bucket decreases with the increase of the penetration depth ratio due to the increase of the soil strength with depth. For the foundation with inner bucket and cruciform skirts during the shallow penetration, the  $H_{plug}$  is significantly higher than that of the bucket foundation without compartment. This is due to the added inner bucket and cruciform skirts squeezed more soil during the penetration, which gradually flowed into the inner or outer compartment. As the penetration depth ratio increases (i.e.,  $d_p/D > 0.5$  for the inner compartment and  $d_p/D > 0.8$  for the outer compartment), the  $H_{plug}$  decreases with the increase of the penetration depth ratio. The main reason lies in the larger friction resistance caused by the inner bucket and cruciform skirt, which prevents the soil from flowing into the inner or outer compartment.

Meanwhile, it can be seen from Figure 4 that with further penetration, the difference of the  $H_{plug}$  between the inner and outer compartment becomes greater. Take  $d_p/D = 1.5$  as an example; the  $H_{plug}$  in the outer compartment is about 1.7 m, which prevents the bucket foundation to penetrate into the predetermined depth and correspondingly its post-installation bearing capacity reduces. The  $H_{plug}$  in the outer compartment is about 1.0 m lower than the original mud surface, which greatly decreases the vertical bearing capacity of the foundation due to non-contact between the lid of the bucket and the soil.

The evolution of the soil surface height in each compartment has correlation with the soil flow. Figure 5 is the section view of the soil flow velocity vector at different positions and penetration depths (i.e., the section view is the soil flow along the section 1-1' in Figure 2b). Figure 5a reflects the trend of soil flow during shallow penetration ( $d/D = 0.1$ ). It can be seen that the soil around each skirt flows downwards and then evenly flows to both sides. As the penetration depth increases to  $d/D = 0.5$  in Figure 5b, and since the outer boundary of the bucket is closer to the semi-infinite space and the inner boundary of the bucket is limited, the passive earth pressure inside the bucket is lower than that of

the outside. The soil is more inclined to flow in the compartment. When the penetration depth further increases to  $d/D = 1.5$  in Figure 5c, the contact area between the skirt and the soil also increases. The influence of side friction during the penetration of the foundation cannot be ignored. The larger frictional resistance in the inner and outer compartments not only hinders the upward flow of the soil (such as that in the outer compartment), but also pushes a large amount of soil to move downward together (such as that in the inner compartment).

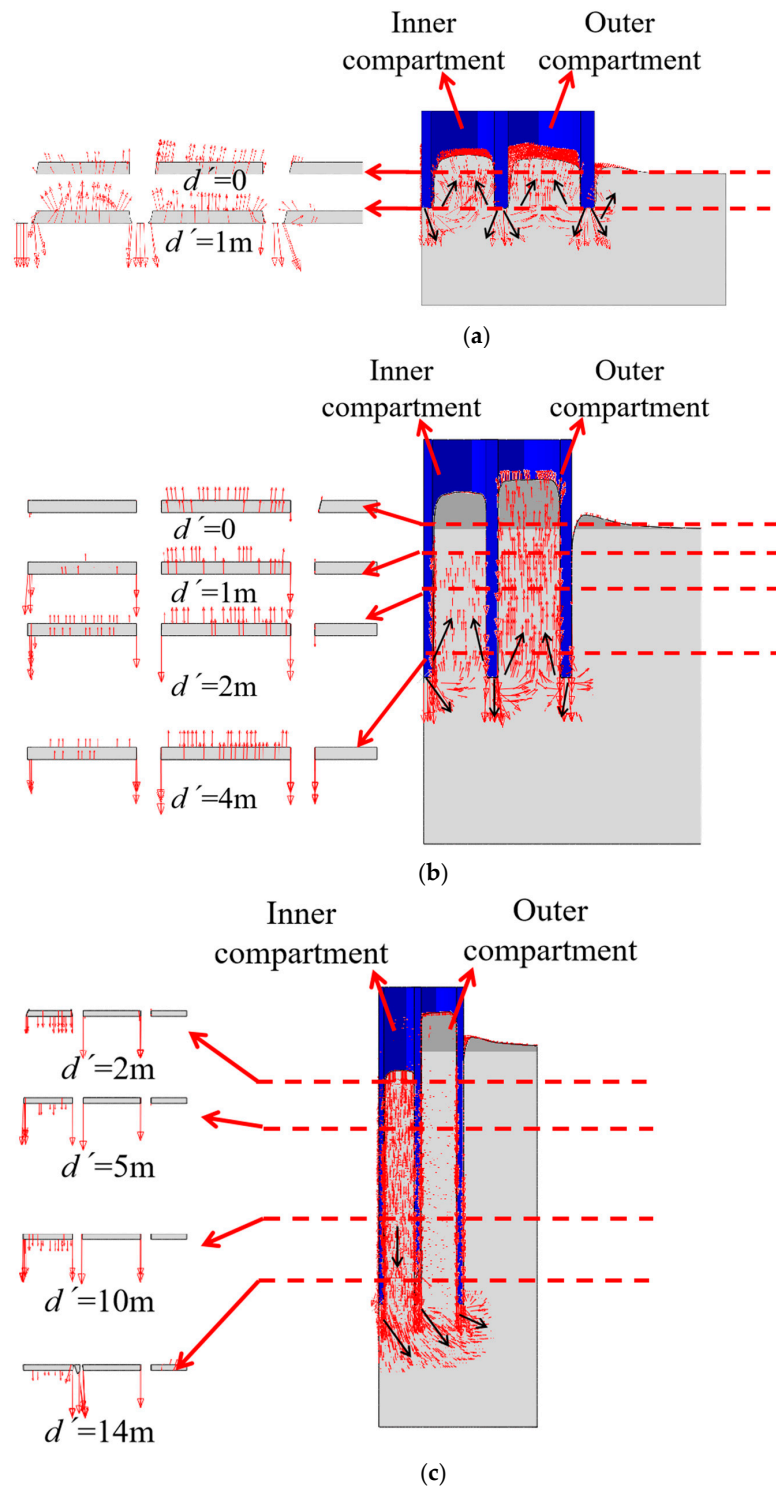


**Figure 5.** Soil flow at the penetration depth ratio of  $d/D = 0.1, 0.5$  and  $1.5$ . (a)  $d/D = 0.1$ . (b)  $d/D = 0.5$ . (c)  $d/D = 1.5$ .

### 3.2. Penetration Resistance

Take  $d/D = 1$  as an example, the total penetration resistances of the bucket foundation with inner bucket and cruciform skirts and those of the hollow bucket foundation calculated by the CEL model in this study and the method in Housby and Byrne (2005) are shown in Figure 6. Due to the inclusion of the internal cylindrical and the cruciform skirts, the bucket foundation has a significantly higher penetration resistance than the hollow bucket foundation.

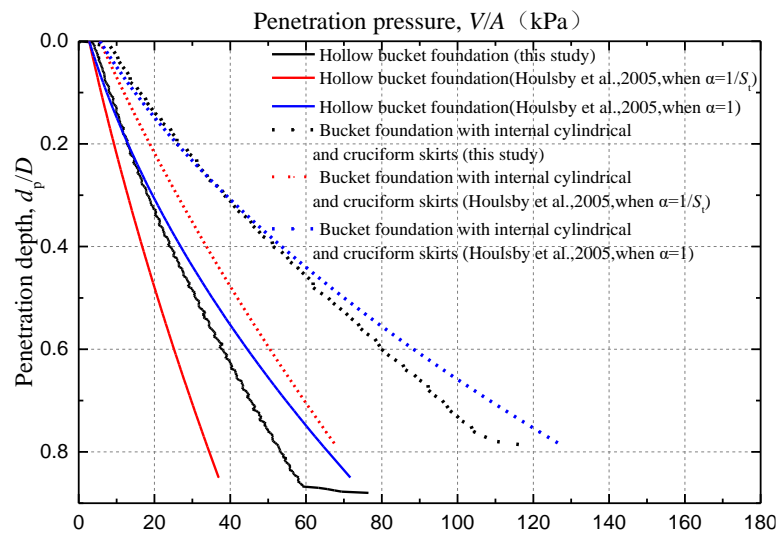


Figure 6. The total penetration resistances with the increase of penetration depth [24].

When the foundation was installed to a certain depth, it can be seen from the CEL results in Figure 6 that the penetration resistance suddenly changed, which is due to the soil heave inside the compartment. When the soils inside the bucket started to contact the bucket lid, the installation resistance suddenly increased, which affects the subsequent penetration of the bucket. As the bucket cannot be installed into the design depth, the in-place stability of the bucket foundation will be affected.

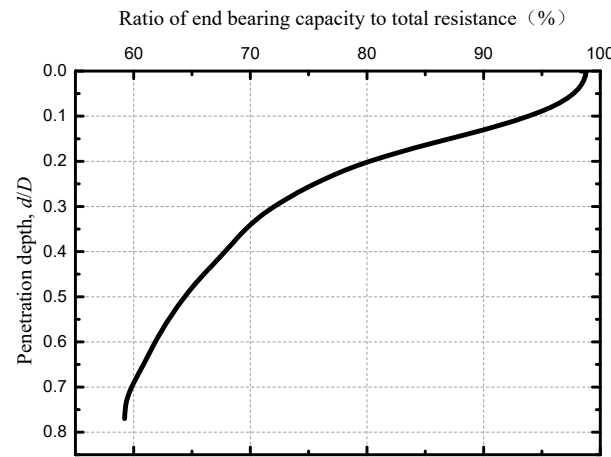
Housby and Byrne [24] studied the penetration resistance of hollow bucket foundations based on the theory of limit equilibrium, for which the penetration resistance is equal to the sum of the side friction resistance and the end bearing capacity at the bottom of the skirts. The theoretical calculation expression of the penetration resistance for the bucket foundation was proposed as:

$$V' = d\alpha_0 s_{u0,av}(\pi D) + d\alpha_i s_{u0,av}(\pi D_i) + (\gamma' dN_q + s_{u0,tip} N_c)(\pi D't) \quad (5)$$

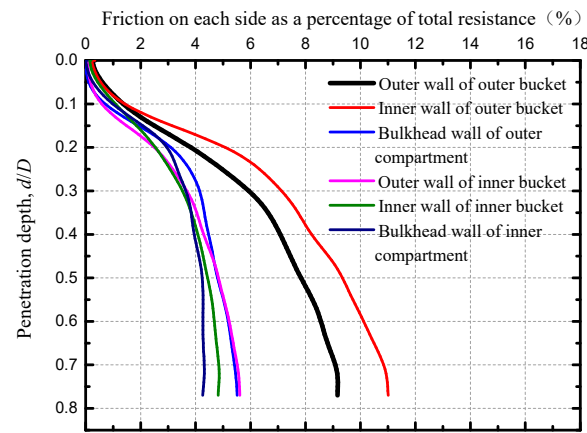
where  $V'$  is the total penetration resistance of the foundation;  $D_i$  and  $D'$  are the internal diameter of the bucket and the average diameter of the bucket; hence,  $\pi D't$  is approximately equal to the area of the foundation bottom;  $d$  is the penetration depth;  $\alpha_0$  and  $\alpha_i$  are the adhesion coefficients of the frictional resistance on the outer skin and inner skin of the bucket, respectively;  $s_{u0,av}$  is the soil average intact undrained shear strength over the penetration depth, while  $s_{u0,tip}$  is the soil intact undrained shear strength at the skirt tip level; and  $N_c$  is the end bearing capacity coefficient of the deep strip foundation in the clay [25]. For undrained soft soil,  $N_q = 1$ . The predicted results obtained from the equation proposed by Housby and Byrne [24] are shown in Figure 6. The results obtained from the formula proposed by Housby and Byrne [24] when  $\alpha_0 = \alpha_i = 1/S_t$  are smaller than the CEL results, which is mainly because the soil is considered as the fully-remolded soil after the penetration of the bucket foundation. When no strain softening is considered for the soil, i.e., when  $\alpha_0 = \alpha_i = 1$ , the results calculated by the equation proposed by Housby and Byrne [24] are larger than the finite element results in this study. However, a portion of soils should be considered as in a partially-remolded condition. Therefore, the penetration

resistance of the bucket foundation in clay accounting for a partially-remolded condition in this study is more reasonable.

Although the bucket foundation studied in this paper incorporates the inner bucket and cruciform skirts, its penetration resistance can still be calculated according to the theory proposed by Houlsby and Byrne [24]. The ratio of the individual resistance to the total resistance of the bucket foundation with the inner bucket and cruciform skirts is shown in Figure 7.



(a)



(b)

**Figure 7.** Proportion of resistance to total resistance. (a) Ratio of end bearing capacity to total resistance. (b) Percentage of friction on each part.

It can be seen that the total resistance of the concrete thick-wall bucket foundation with the inner bucket and cruciform skirts mainly comes from the end bearing capacity. The ratio of the friction resistance to total penetration resistance increases with the penetration depth.

### 3.2.1. End Bearing Capacity

The equation for calculating the end bearing capacity at the bottom of the bucket is:

$$F_N = (\gamma'dN_q + s_{u0,tip}N_c)A \tag{6}$$

where  $A$  is the bottom area. Therefore, the end bearing capacity coefficient  $N_c$  can be derived as:

$$N_c = \left( \frac{F_N}{A} - \gamma' d N_q \right) / s_{u0,tip} \tag{7}$$

For the hollow bucket foundation and the bucket foundation with inner bucket and cruciform skirts, the corresponding change of the end bearing capacity coefficient  $N_c$  with the penetration depth ratio is shown in Figure 8.

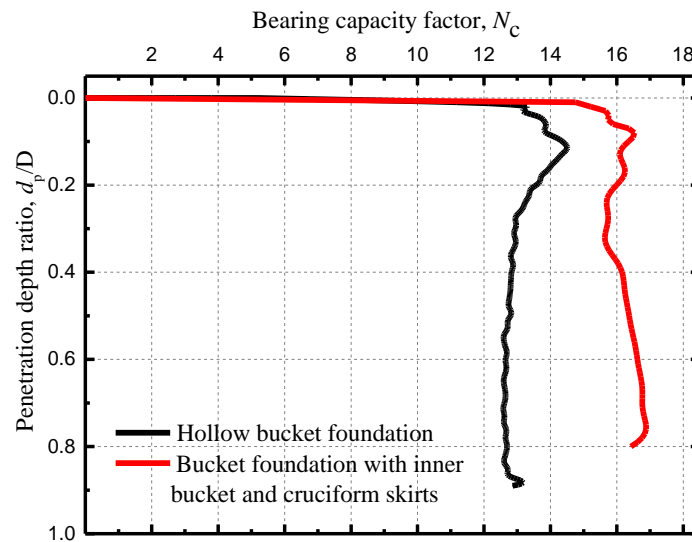


Figure 8. End bearing capacity coefficient  $N_c$ .

It can be seen from Figure 8 that the end bearing capacity coefficient of the hollow bucket foundation first increases with the penetration depth and then slightly decreases before stabilizing during further penetration. For bucket foundations with inner bucket and cruciform skirts, after the end bearing capacity coefficient increases and then slightly decreases with penetration depth, a slight increase occurs with penetration depth. For the investigated penetration depth, the end bearing capacity coefficient of the bucket foundation with inner bucket and cruciform skirts is obviously greater than that of the hollow bucket foundation.

### 3.2.2. Skirt Friction

According to Equation (5), the Equation for calculating skirt friction is shown as Equation (8):

$$F_f = d\alpha s_{u0,av} L \tag{8}$$

where  $L$  is the perimeter or width of each skirt. After conversion, the Equation for the adhesion coefficient  $\alpha$  is:

$$\alpha = F_f / d s_{u0,av} L \tag{9}$$

The adhesion coefficient  $\alpha$  between the skirting board and the soil on both sides are calculated and the results for each skirt are shown in Table 2.

Table 2. Adhesion coefficient for each skirt.

Outer Wall of Outer Bucket	Inner Wall of Outer Bucket	Bulkhead Wall of Outer Compartment
0.51	0.68	0.60
Outer wall of inner bucket	Inner wall of inner bucket	Bulkhead wall of inner compartment
0.70	0.79	0.63

The adhesion coefficient is generally considered as the inverse of the sensitivity of the soil, for which it is 0.25 in this case. However, it can be seen from the table that the value is much larger than 0.25 because the soil was partially remolded during the installation.

The adhesion coefficient  $\alpha$  on the side of the skirting board is mainly determined by the degree of disturbance to the soil during the foundation installation, which can be expressed by the softening coefficient. However, for bucket foundations with inner bucket and cruciform skirts, the soil height in the compartment is too large due to the relatively small height of the foundation, which increases the adhesion coefficient.

Taking the penetration depth ratio  $d/D = 0.5$  as an example, the section view of the softening factor of the soil is shown in Figure 9. The corresponding softening factor of the soil near different skirting boards is shown in Figure 10.

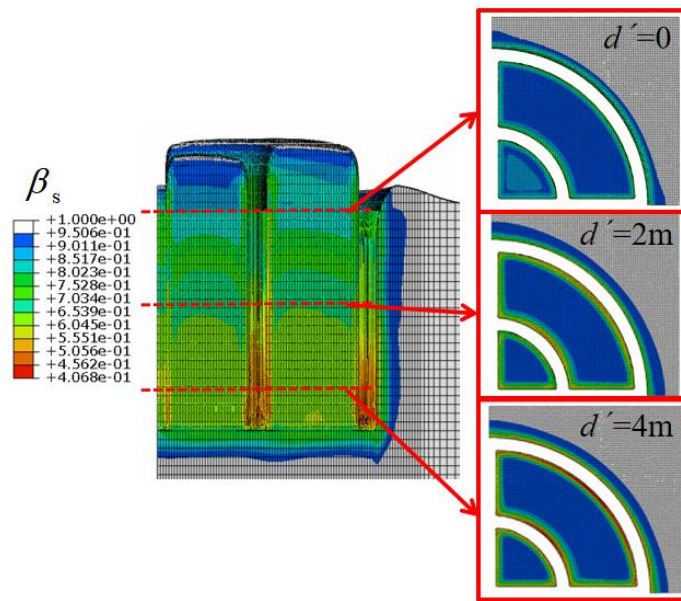


Figure 9. Section view of soil softening factor at different depths.

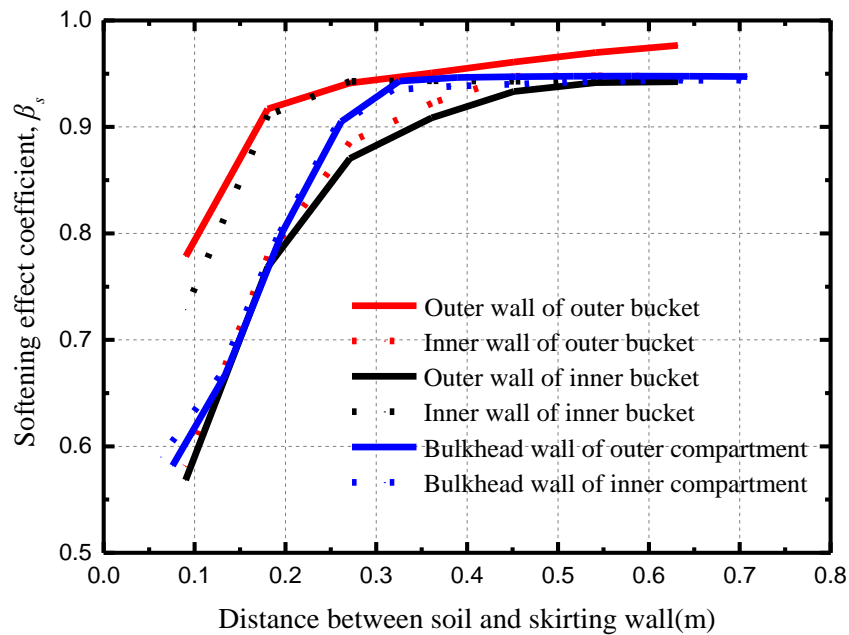


Figure 10. Softening factor of soil for each skirt.

It can be seen that the deeper the depth, the more severe the softening effect. Among the different skirting walls, most softening occurred in the outer wall of the inner bucket. However, due to the larger volume of soil in the outer compartment, the cohesion coefficient for the inner wall of the inner bucket is the largest while the cohesion coefficient of the outer wall of the outer bucket is the smallest.

### 3.3. The Optimal Inner Bucket Diameter

Through the analysis of soil flow and soil plug during the penetration, it is found that  $D_{in} = D/2$  is not the optimal configuration based on the analysis of the soil plug inside the foundation after penetration, though the contribution of the inner bucket to improve the overall rigidity of the foundation can be maximized. When the penetration depth is relatively large, the excessive difference in soil height between the inner and outer compartments will adversely affect the bearing capacity of the foundations.

It is feasible to vary the diameter of the inner bucket to affect the soil flow, so that a part of the soil that originally flowed into the outer compartment can be diverted to the inner compartment and maintained similar height of soil. It can not only solve the negative height of the soil in the inner compartment, but also reduce the height of the soil in the outer compartment. It is more conducive to the installation of the foundation to the predetermined buried depth and to achieving the designed bearing capacity.

Based on previous analysis, for large penetration depth, the side friction resistance of the unit volume of the soil in the compartment will play a decisive role in the flow of the soil and the final height of the soil in the compartment. In order to ensure similar soil height for the inner and outer compartments, the total lateral friction resistance acting on the unit volume of the soil should be equal in the inner and outer compartments. This is expressed in Equation (10):

$$\frac{F_{fin}}{V_{in}} = \frac{F_{fout}}{V_{out}} \tag{10}$$

where  $F_{fin}$  and  $F_{fout}$  are the total friction of the soil in the inner and outer compartments, and it has correlation to the coefficient of side friction, the average soil shear strength over the penetration depth, the bottom perimeter of the compartment, and the penetration depth, as shown in Equation (8);  $V_{in}$  and  $V_{out}$  are the soil volumes in the compartments, and they can be expressed by the bottom area of the compartments and the penetration depth. During the penetration of the bucket foundation with inner bucket and cruciform skirts, the penetration depth and the average soil shear strength are equal in the inner and outer compartments. Based on previous analyses, the side friction coefficients of the skirts are similar. For the convenience of analysis, it can be assumed that the side friction coefficients of the skirts are equal, and Equation (10) is expressed as:

$$\frac{\alpha s_{u0,av} L_{in} d}{S_{in} d} = \frac{\alpha s_{u0,av} L_{out} d}{S_{out} d} \tag{11}$$

It can be simplified to:

$$\frac{L_{in}}{S_{in}} = \frac{L_{out}}{S_{out}} \tag{12}$$

where  $L_{in}$  and  $L_{out}$  are the bottom perimeter of the inner and outer compartment; and  $S_{in}$  and  $S_{out}$  are the bottom area of the inner and outer compartments. The diameter of the inner bucket should be changed so that the inner and outer compartments satisfy Equation (12). Further calculation concluded that when  $a_{in} = a_{out}$ , the diameter of the inner bucket is about 5/8 of the total diameter ( $D_{in} = 5/8D$ ).

In addition, in order to better compare the influence of the diameter of internal cylinder on the soil flow and the soil surface in the inner and outer compartments during the foundation penetration process, it is necessary to calculate the penetration model when the diameter of the inner bucket is 3/4 of the total diameter.

When  $D_{in} = 1/2D$ ,  $5/8D$ , and  $3/4D$ , the average height of the soil surface and soil flow in the inner and outer compartments at different penetration depths (the 1-1' section in Figure 2b) are shown in Figure 11. It can be seen that by changing the diameter of the inner bucket, the trend of soil flow changes significantly, and at the theoretically optimal inner bucket diameter (i.e.,  $D_{in} = 5/8D$ ), the inner and outer compartments can maintain similar soil surface. However, if the diameter of the inner cylinder is too large (i.e.,  $D_{in} = 3/4D$ ), the soil in the outer compartment will appear to have a negative height due to the excessive friction when the penetration depth is relatively large.

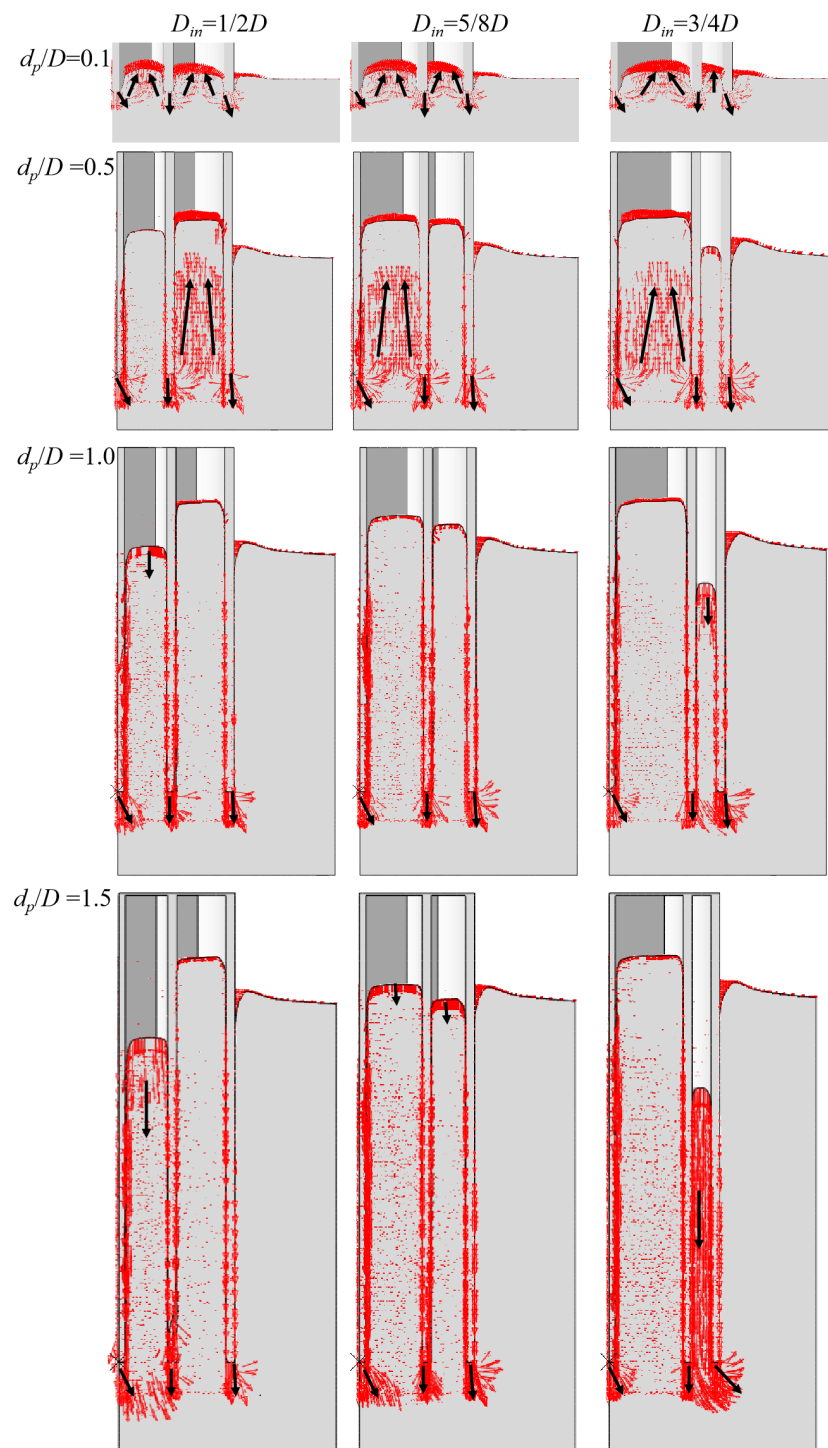


**Figure 11.** The height of the soil surface and soil flow in the inner and outer compartments under different inner bucket diameters and penetration depths.

#### 4. Conclusions

In this paper, a CEL large-deformation finite element model was established to simulate the penetration of the bucket foundation with inner bucket and cruciform skirts. The soil strain softening effect was considered. The soil flow, soil strength evolution, and penetration resistance during the installation were investigated. Then, the optimal inner bucket diameter was suggested based on the theoretical analysis and numerical results. The main findings are as follows:

(1) Due to the addition of inner bucket and cruciform skirts, the average height of the soil surface inside the inner or outer compartment is significantly higher than that of the hollow bucket foundation during shallow penetration. However, if the adopted diameter of the inner bucket is half the diameter of the outer bucket, the larger frictional resistance in the outer compartment hinders the upward flow of the soil with the increase of the penetration depth, while that in the inner compartment a large amount of soil is pushed downward. The significant difference of soil height between the outer and inner compartment will affect the post-installation bearing capacity of the foundation.

(2) The total resistance of a concrete thick-walled bucket foundation with the inner bucket and cruciform skirts is equal to the sum of the friction resistance of all skirts and the end bearing capacity. The end bearing capacity coefficient of the bucket foundation with the inner bucket and cruciform skirts was significantly larger than that of the hollow bucket foundation. Meanwhile, the end bearing capacity accounts for a large proportion of the total resistance. Due to the partial remolding of the soil during the penetration, the friction coefficient for the bucket skirt was larger than the inverse of the sensitivity of the soil.

(3) The optimal inner bucket diameter is equal to 5/8 of the outer diameter obtained from the theoretical analysis and numerical results. Under the circumstances, the height of the soil surface in the inner and outer compartments is almost equal because the friction resistance acting on the unit volume of the soil in the inner compartment is equal to that in the outer compartment. It can be seen that the trend of soil flow is effectively varied by expanding the ratio of the diameter of the inner bucket to the outer diameter of the bucket foundation.

The findings add further value to the application of multi-compartment foundations such as bucket foundations with internal cylindrical and cruciform skirts. Further investigation is necessary to study the penetration of the bucket foundation, equipped with an inner bucket and cruciform skirts, into sandy soil, while taking into account the staged installation and variation in pore pressure.

**Author Contributions:** Conceptualization, Z.X.; methodology, Z.X. and T.M.; software, Z.X. and T.M.; validation, Z.X. and T.M.; formal analysis, Z.X. and T.M.; investigation, Z.X. and T.M.; resources, Z.X.; data curation, Z.X.; writing—original draft preparation, Z.X. and T.M.; writing—review and editing, Z.X. and P.H.; visualization, Z.X. and T.M.; supervision, Z.X., H.W., F.B., H.J., T.Y., W.Z., P.H. and J.L.; project administration, Z.X. and T.Y.; funding acquisition, Z.X., H.W., F.B., H.J., P.H. and J.L. All authors have read and agreed to the published version of the manuscript.

**Funding:** This research was funded by the National Key Research and Development Program of China (No. 2021YFB2600200) and the National Natural Science Foundation of China (No. 51879187; No. 51979067; No. 51890915).

**Institutional Review Board Statement:** Not applicable.

**Informed Consent Statement:** Not applicable.

**Data Availability Statement:** Data is contained within the article.

**Conflicts of Interest:** The authors declare no conflict of interest.

## Notation

$D$	Outer diameter of bucket foundation
$d$	Skirt depth
$d_p$	Penetration depth
$s_u$	Undrained soil shear strength
$\gamma'$	Submerged unit weight
$E$	Young's modulus
$\nu$	Poisson's ratio
$S_t$	Soil sensitivity
$\beta_s, \beta_r$	Soil strain softening and rate factors
$\delta_{rem}$	Reciprocal of soil sensitivity, $= 1/S_t$
$\xi$	Current accumulated absolute plastic shear strain
$\epsilon_1, \epsilon_3$	Major and minor principal total strains
$H_{plug}$	Average height of soil surface relative to original mud surface in bucket foundation
$V'$	Penetration resistance
$N_c$	End bearing capacity factor
$\alpha$	Frictional coefficient
$\alpha_0, \alpha_i$	Outer skin and inner skin frictional coefficient
$\xi_{95}$	Soil relative ductility (value of $\xi$ for the undrained shear strength to achieve 95% remoulding)
$s_{u0,av}$	Soil average intact undrained shear strength over the penetration depth
$s_{u0,tip}$	Soil intact undrained shear strength at the skirt tip level
$d'$	Depth for a position under the same penetration depth
$D_{in}$	Diameter of the inner bucket
$F_{fin}, F_{fout}$	Total friction of the soil in the inner and outer compartments
$S_{in}, S_{out}$	Bottom areas of the inner and outer compartments
$L_{in}, L_{out}$	Bottom perimeter of the inner and outer compartments

## References

- Xiao, Z.; Liu, Y.; Ge, B.; Fu, D.F.; Zhou, Z.F.; Yan, Y. Bearing performance of offshore bucket foundation with internal cruciform skirt under combined loading. *Mar. Georesour. Geotechnol.* **2020**, *38*, 1209–1222. [\[CrossRef\]](#)
- Tjelta, T.I. Geotechnical Experience from the Installation of the Europipe Jacket with Bucket Foundations. In Proceedings of the Offshore Technology Conference, Houston, TX, USA, 1–4 May 1995; pp. 897–908.
- Iskander, M.; El-Gharbawy, S.; Olson, R. Performance of Suction Caissons in Sand and Clay. *Can. Geotech. J.* **2002**, *39*, 576–584. [\[CrossRef\]](#)
- Chen, W.; Randolph, M. Radial Stress Changes around Caissons Installed in Clay by Jacking and by Suction. In Proceedings of the Fourteenth International Offshore and Polar Engineering Conference, Toulon, France, 23–28 May 2004; pp. 493–499.
- Zhai, H.; Zhang, P.; Ding, H.; Le, C.; Wei, W. Laboratory tests on measures of reducing penetration resistance in bucket foundation installation. *Mar. Georesour. Geotechnol.* **2021**, *39*, 929–936. [\[CrossRef\]](#)
- Wang, Y.; Zhu, X.; Lv, Y.; Yang, Q. Large Deformation Finite Element Analysis of the Installation of Suction Caisson in Clay. *Mar. Georesour. Geotechnol.* **2018**, *36*, 883–894. [\[CrossRef\]](#)
- Xiao, Z.; Fu, D.; Zhou, Z.; Lu, Y.; Yan, Y. Effects of strain softening on the penetration resistance of offshore bucket. *Ocean. Eng.* **2019**, *193*, 106594. [\[CrossRef\]](#)
- Xiao, Z.; Lu, Y.M.; Wang, Y.Z.; Tian, Y.H.; Zhao, Y.B.; Fu, D.F.; Zhang, D.H. Investigation into the influence of caisson installation process on its capacities in clay. *Appl. Ocean. Res.* **2020**, *104*, 102370. [\[CrossRef\]](#)
- Jin, Z.; Yin, Z.; Kotronis, P.; Jin, Y.F. Numerical Investigation On Evolving Failure of Caisson Foundation in Sand Using the Combined Lagrangian-SPH Method. *Mar. Georesour. Geotechnol.* **2019**, *37*, 23–35. [\[CrossRef\]](#)
- Liu, R.; Chen, G.; Lian, J.; Ding, H. Vertical Bearing Behaviour of the Composite Bucket Shallow Foundation of Offshore Wind Turbines. *J. Renew. Sustain. Energy* **2015**, *7*, 13123. [\[CrossRef\]](#)
- Zhang, P.; Guo, Y.; Liu, Y.; Ding, H. Experimental Study On Installation of Hybrid Bucket Foundations for Offshore Wind Turbines in Silty Clay. *Ocean. Eng.* **2016**, *114*, 87–100. [\[CrossRef\]](#)
- Ghosh, S.; Kikuchi, N. An Arbitrary Lagrangian-Eulerian Finite Element Method for Large Deformation Analysis of Elastic-Viscoplastic Solids. *Comput. Methods Appl. Mech. Eng.* **1991**, *86*, 127–188. [\[CrossRef\]](#)
- Simulia, D. *ABAQUS Version 6.13. Analysis User's Manual*; Abaqus 6.13 Documentation; Dassault Systèmes Inc.: Providence, RI, USA, 2013.
- Chen, W.; Zhou, H.; Randolph, M.F. Effect of installation method on external shaft friction of caissons in soft clay. *J. Geotech. Geoenviron. Eng.* **2009**, *135*, 605–615. [\[CrossRef\]](#)

15. Zhou, H.; Randolph, M.F. Large deformation analysis of suction caisson installation in clay. *Can. Geotech. J.* **2006**, *43*, 1344–1357. [[CrossRef](#)]
16. Chen, W.; Randolph, M.F. External radial stress changes and axial capacity for suction caissons in soft clay. *Géotechnique* **2007**, *57*, 499–511. [[CrossRef](#)]
17. Zhang, Y.; Wang, D.; Cassidy, M.J.; Bienen, B. Effect of installation on the bearing capacity of a spudcan under combined loading in soft clay. *J. Geotech. Geoenviron. Eng.* **2016**, *140*, 04014029. [[CrossRef](#)]
18. Vulpe, C.; Gourvenec, S.; Power, M. A generalised failure envelope for undrained capacity of circular shallow foundations under general loading. *Géotech. Lett.* **2014**, *4*, 187–196. [[CrossRef](#)]
19. Vulpe, C. Design method for the undrained capacity of skirted circular foundations under combined loading: Effect of deformable soil plug. *Géotechnique* **2015**, *65*, 669–683. [[CrossRef](#)]
20. Einav, I.; Randolph, M.F. Combining upper bound and strain path methods for evaluating penetration resistance. *Int. J. Numer. Methods Eng.* **2005**, *63*, 1991–2016. [[CrossRef](#)]
21. Liu, H.; Xu, K.; Zhao, Y. Numerical investigation on the penetration of gravity installed anchors by a coupled Eulerian—Lagrangian approach. *Appl. Ocean. Res.* **2016**, *60*, 94–108. [[CrossRef](#)]
22. Randolph, M.F. Characterization of soft sediments for offshore applications. In Proceedings of the 2nd International Conference on Site Characterization, Millpress Science, Rotterdam, The Netherlands, 19–22 September 2004; pp. 209–231.
23. Westgate, Z.J.; Tapper, L.; Lehane, B.M.; Gaudin, C. Modelling the installation of stiffened caissons in overconsolidated clay. In Proceedings of the ASME 28th International Conference on Ocean, Offshore and Arctic Engineering, Honolulu, HI, USA, 31 May–5 June 2009; pp. 119–126.
24. Housby, G.T.; Byrne, B.W. Design procedures for installation of suction caissons in clay and other materials. *Proc. Inst. Civ. Eng. Geotech. Eng.* **2005**, *158*, 75–82. [[CrossRef](#)]
25. Det Norske Veritas. Geotechnical design and installation of suction anchors in Clay. In Proceedings of the Offshore Technology Conference-Asia, Houston, TX, USA, 2–5 May 2005. Recommended practice E303.

**Disclaimer/Publisher’s Note:** The statements, opinions and data contained in all publications are solely those of the individual author(s) and contributor(s) and not of MDPI and/or the editor(s). MDPI and/or the editor(s) disclaim responsibility for any injury to people or property resulting from any ideas, methods, instructions or products referred to in the content.